4. Comparison of Cs_2MX_4 Crystals of the β-K_2SO_4-type Structure with and without the IC Phase -Microscopic Mechanisms Inducing the IC Phase Transition-

4.1 Introduction

In chapter 2, dynamic properties in N-IC phase transitions and of IC phase modulations in Cs_2MX_4 compounds with the β-K_2SO_4-type structure and the IC phase at low temperatures (Cs_2CdBr_4, Cs_2HgBr_4, Cs_2HgCl_4 and modification-A of Cs_2CdI_4) were discussed. In chapter 3, the structural effect was investigated in Cs_2MX_4 compounds with the Sr_2GeS_4-type structure (modification-Bs of Cs_2CdI_4 and Cs_2HgI_4) which undergo no phase transition at low temperatures and with the β-K_2SO_4-type structure (Cs_2ZnCl_4 and Cs_2ZnBr_4) in addition to Cs_2ZnI_4, which shows a different IC phase.

In this chapter, Cs_2MX_4 compounds of the β-K_2SO_4-type structure with and without the IC phase are compared with each other to clarify the microscopic mechanism for the appearance of the IC phase by means of detailed analysis of chemical shifts of ^{133}Cs NMR and quadrupole coupling constants e^2Qq/h and by referring to the theoretical prediction of the appearance of the one-dimensional modulation in the pseudo-spin system.

4. 2 The microscopic mechanism for the one-dimensional modulation in the discrete pseudo-spin system

The appearance of one-dimensionally modulated phase has been predicted theoretically in the discrete pseudo-spin model with short range competing interactions, which is called the axial-next-nearest-neighbor Ising (ANNNI) model [1-4]. If the 2nd neighbor interactions only in the one-dimension along the modulation are considered, the Hamiltonian is given by

$$\hat{H} = -\sum_{i,j} (J_0 S_{i,j} S_{i+1,j} + J_1 S_{i,j} S_{i,j+1} + J_2 S_{i,j} S_{i,j+2}) ,$$

where $S_{i,j}$ denotes the spin in the i-th one-dimensional chain and the j-th layer perpendicular to the chain, J_0 is the interaction between the nearest neighbors in the layer, J_1 is the interaction between the nearest neighbor spins and J_2 is that between the 2nd neighbor spins in the chain as shown in Fig. 4. 1. In the j-th layer perpendicular to the one-dimensional axis, the spins are connected by the ferro-type interaction $J_0 > 0$. In cases of $J_1 > 0$ (ferro-type) and $J_2 < 0$ (antifero-type), the nearest and the 2nd neighbor interactions is competing. Various modulations depending on the ratio $-J_2 / J_1$ appear as the result of the competition [1, 2, 4].

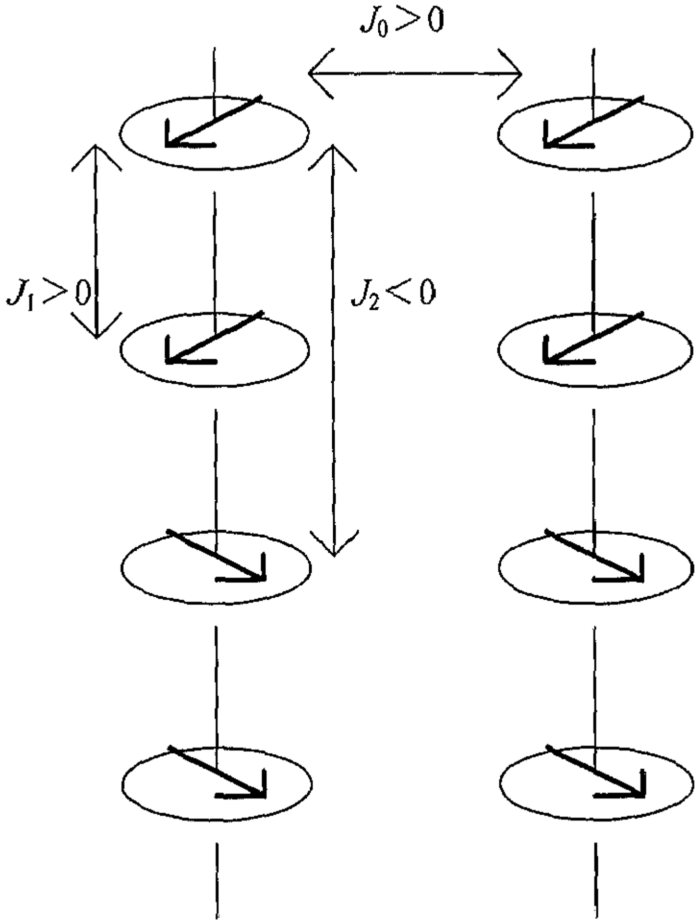

Fig. 4. 1 The axial-next-nearest-neighbor Ising (ANNNI) model in the discrete pseudo-spin (bold arrows) system. $J_0 > 0$ represents the nearest neighbor interaction in the direction perpendicular to the one-dimensional chain and $J_1 > 0$ and $J_2 < 0$ represent the nearest neighbor and the 2nd neighbor interactions, respectively, along the chain.

4. 3 Experimental Results and Discussion

The values of chemical shifts of ^{133}Cs NMR in Cs_2MX_4 compounds with the IC phase at 300 K were evaluated from central peak frequencies taking into account the anisotropy and the 2nd order shift caused by the nuclear quadrupole interaction (Table 4. 1). Temperature dependences of the chemical shifts in these compounds are shown in Fig. 4. 2. For all Cs_2MX_4 compounds studied in this chapter, ^{133}Cs NMR lines observed on the low-frequency side, which has e^2Qq/h and η values smaller than those of the other high-frequency one, was assigned to the Cs1 site (Fig. 2. 7), because the e^2Qq/h and η values estimated for this line from the crystal structure showed that the Cs site is a symmetry higher than that of the other one. The Cs1 ions are alternately stacked with complex anions and considered to play the role of connectng anions one-dimensionally along *a*-axis (Fig. 4. 3), while the Cs2 sites are in the *bc*-plane (Fig 4. 3).

Table 4. 1 Chemical shifts estimated from peak frequencies which are corrected using the anisotropy of chemical shifts in the central lines and the 2nd order perturbed shifts given by eq. (3.6) in Cs_2MX_4 compounds.

Compounds	Peak Frequency / Hz	Frequency Correction / Hz		Chemical Shift / ppm
		Anisotropy of Chemical Shift	2nd Order Shift	
Cs_2CdBr_4	2217	+1000	+ 5	82
	6676	+ 50	+12	171
Cs_2HgBr_4	2073	+1110	+ 4	81
	6862	+ 50	+14	176
Cs_2CdI_4	2663	± 0	+ 4	68
	7184	+ 500	+16	195
Cs_2HgCl_4	1177	+ 500	+ 4	43
	5278	+ 300	+ 9	142

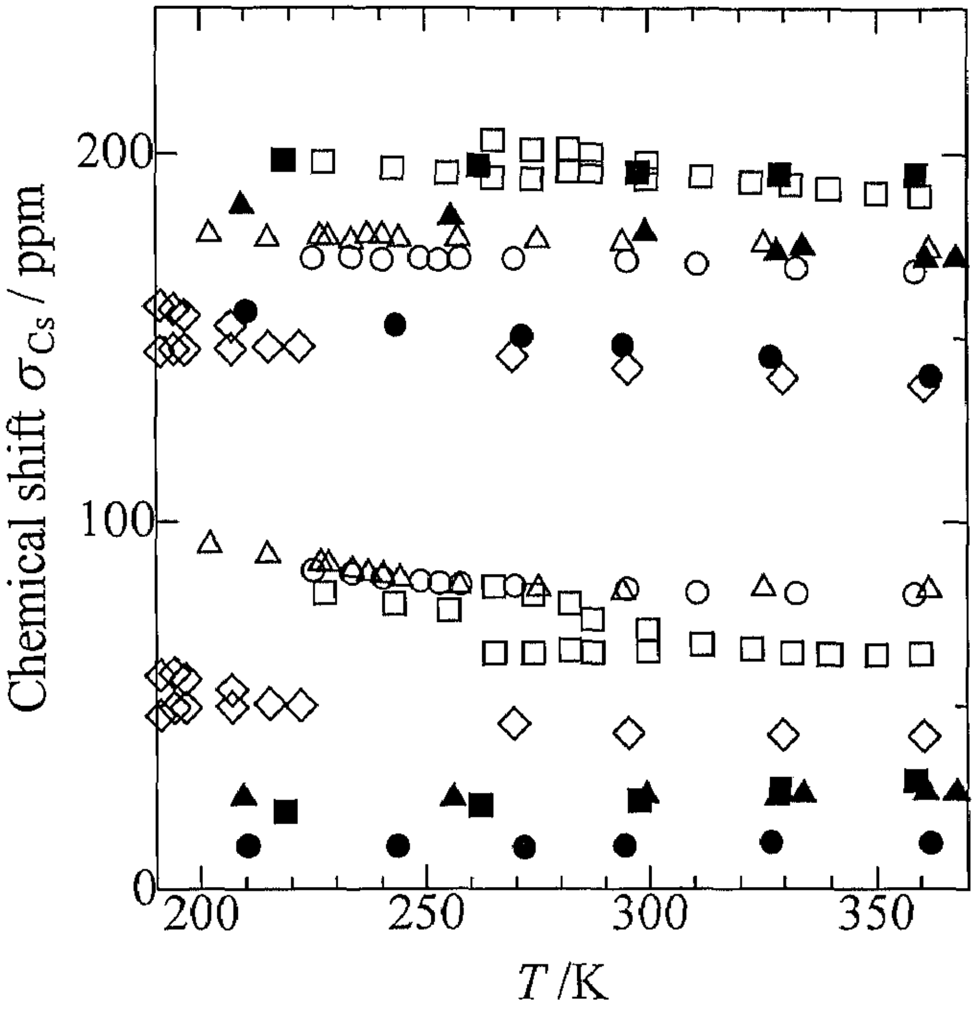

Fig. 4. 2 Temperature dependences of chemical shifts observed in ^{133}Cs NMR spectra in Cs_2MX_4 compounds with β-K_2SO_4-type structure for Cs_2CdBr_4 (○), Cs_2HgBr_4 (△),and Cs_2CdI_4 (□) and Cs_2HgCl_4 (◇) with IC phases, and Cs_2ZnCl_4 (●), Cs_2ZnBr_4 (▲) and Cs_2ZnI_4 (■) without the phase.

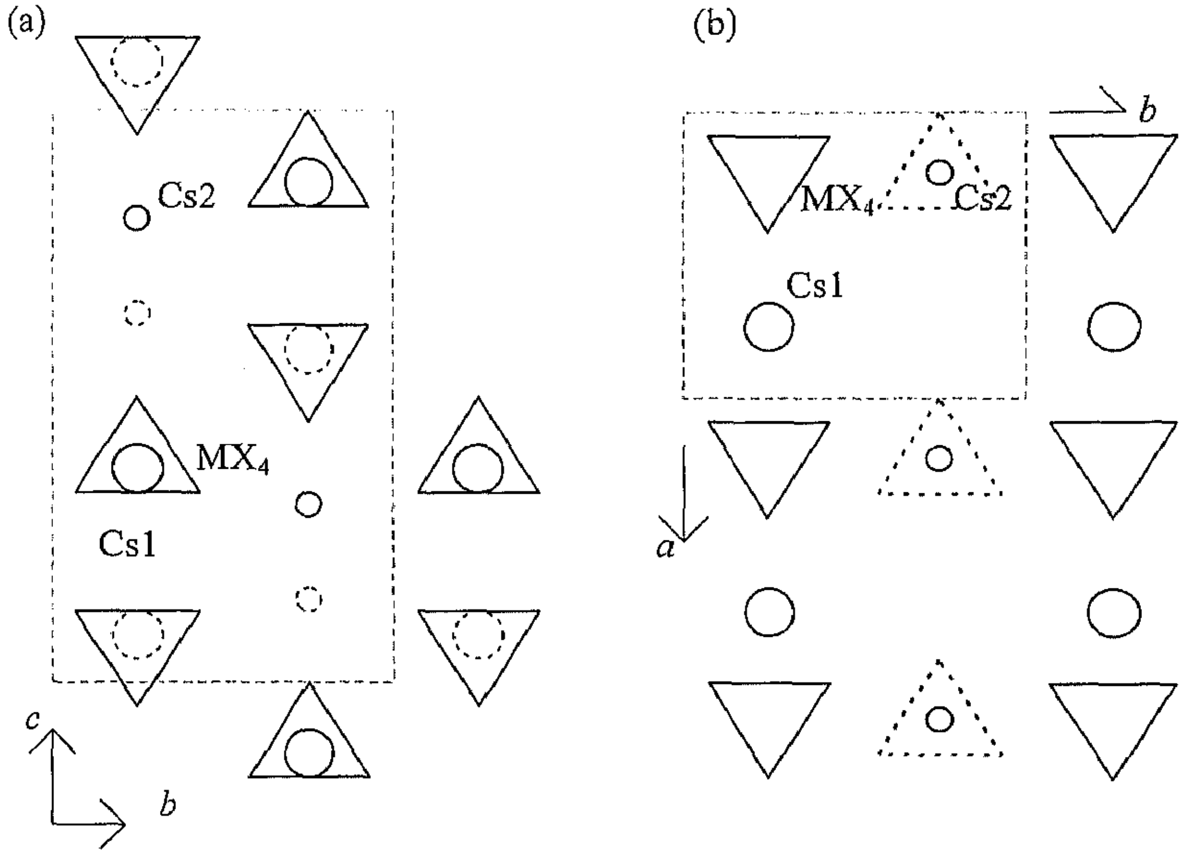

Fig. 4. 3 Schematic crystal structures projected on *bc*- and *ab*-planes. Triangles, large and small circles represent MX_4^{2-} complex anions, Cs1 and Cs2 ions, respectively.

The origin of large differences in chemical shifts between Cs1 and Cs2 sites is considered to be the total degrees of covalency λ in Cs-halogen interactions. The λ values in Cs_2MX_4 compounds were roughly estimated by the foregoing method using eqs. (3.11)-(3.14). The values of covalency λ estimated at *ca.* 300 K are listed in Table 4. 2, where values for Cs_2ZnX_4 are duplicated from Table 3. 7, and temperature dependences of λ are shown in Fig. 4. 4. Comparing the covalency λ values evaluated in the Cs_2MX_4 compounds, it is clarified that: 1) Covalencies of Cs1 are clearly different in Cs_2MX_4 compounds with and without the IC phase. (Cs_2ZnI_4 whose IC phase is different from others, however, will be excluded from the compounds with IC phases and discussed together with Cs_2ZnCl_4 and Cs_2ZnBr_4, which are compounds without the IC phase, in the following section.) 2) Covalencies of Cs2 show inappreciably differences between these compounds. These results suggest that the one-dimensional interaction along *a*-axis through the covalency of Cs1-X interaction affects extremely to the appearance of the IC phase.

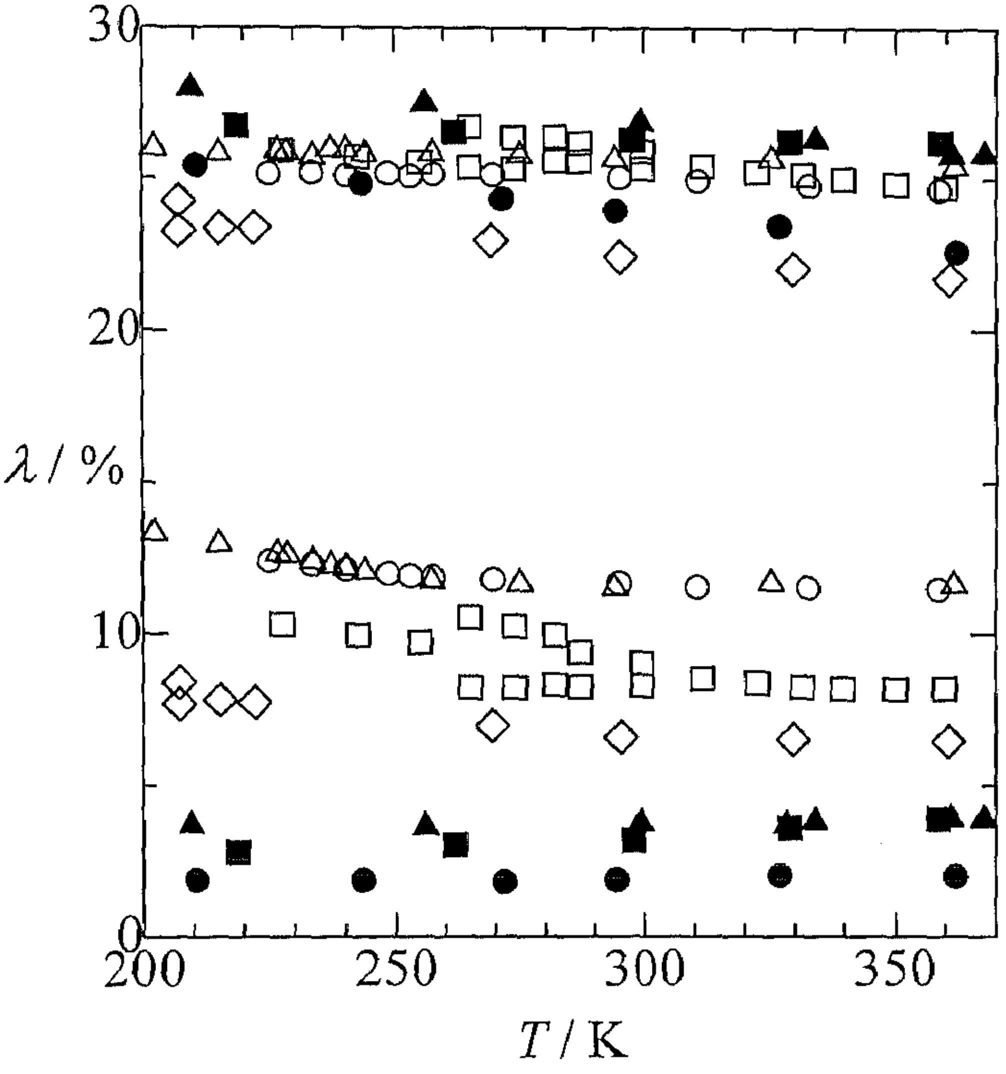

Fig. 4. 4 Temperature dependences of covalencies λ of Cs determined in Cs_2MX_4 compounds with β-K_2SO_4-type structure for Cs_2CdBr_4 (○), Cs_2HgBr_4 (△),and Cs_2CdI_4 (□) and Cs_2HgCl_4 (◇) with IC phases, and Cs_2ZnCl_4 (●), Cs_2ZnBr_4 (▲) and Cs_2ZnI_4 (■) without the phase.

Table 4. 2 The degrees of covalency λ of Cs ions estimated from the chemical shifts in Cs_2MX_4 compounds. ΔE given by eqs. (3.12)-(3.14) taken into account the Born-Mayer repulsion potential and the reported value $\langle 1/r^3 \rangle_p a_0^3$ [5] and the calculated $\langle 1/r^3 \rangle_{d,f} a_0^3$ are used.

Compound	Structure	σ/ppm	ΔE / eV	λ / %
Cs_2ZnCl_4	β-K_2SO_4	12, 148	9.18	2, 24
Cs_2ZnBr_4		25, 179	8.54	4, 27
Cs_2ZnI_4		24, 195	7.66	3, 26
Cs_2HgCl_4	β-K_2SO_4	43, 142	8.99	7, 22
Cs_2CdBr_4		84, 168	8.32	12, 25
Cs_2HgBr_4		82, 174	8.29	12, 25
Cs_2CdI_4		65, 193	7.44	8, 25

This speculation is considered to be supported by the results of thermal expansions and halogen NQR frequencies as mentioned below. At first, the coefficients of linear expansion were estimated from temperature dependences of lattice parameters in N phases in Cs_2MX_4 compounds with the β-K_2SO_4-type structure as listed in Table 4. 3. The coefficients $\overline{\alpha}_a$ in the N phase in Cs_2MX_4 compounds which have the IC phase are larger than that in Cs_2ZnX_4 without IC phase in the low-temperature side. This implies that the interaction along a-axis is getting stronger with temperature decrease in the former compounds than in the later. This result is considered to be consistent with the result reported by Nakayama *et al.* that the closer packing of anions along *a*-axis of a unit lattice drives these compounds to undergo phase transitions on cooling [6]. The consistent results to this packing along *a*-axis were observed as the ratio $a / V^{1/3}$ by Xray powder diffraction and listed in Table 4. 3. The lattice length a is about 2 % shorter than the cube root of the unit lattice volume $V^{1/3}$ in each Cs_2MX_4 compound with the IC phase, though a is nearly equal to $V^{1/3}$ in compounds without the IC phase.

Table 4. 3 Averaged coefficients of liner expansions $\overline{\alpha}_a$, $\overline{\alpha}_b$ and $\overline{\alpha}_c$ along a-, b- and c-axis, respectively, and that of cubical expansion $\overline{\alpha}_V$ in the listed temperature regions, and the lattice length a to the cube root of the unit lattice volume V, a / $V^{1/3}$, at the lowest temperature observed in the N phase with the β-K_2SO_4-type structure.

Compound	Temperature	$\overline{\alpha}_a$ / 10^{-6} K^{-1}	$\overline{\alpha}_b$ / 10^{-6} K^{-1}	$\overline{\alpha}_c$ / 10^{-6} K^{-1}	$\overline{\alpha}_V$ / 10^{-6} K^{-1}	a / $V^{1/3}$
Cs_2ZnCl_4	180 - 360 K	11.6	41.9	37.4	91.1	1.000
Cs_2HgCl_4	220 - 360 K	47.6	40.0	53.2	107.8	0.977
Cs_2ZnBr_4	180 - 330 K	28.9	51.5	61.4	147.5	1.002
	330 - 360 K	-45.8	51.5	61.4	18.5	
Cs_2CdBr_4	252 -360 K	46.1	102.2	36.9	172.0	0.983
Cs_2HgBr_4	244 - 300 K	184.8	41.0	35.8	258.5	0.985
	300 - 360 K	-55.5	41.0	35.8	19.6	
Cs_2ZnI_4	180 - 300 K	-56.0	69.3	39.8	50.1	1.001
	300 - 360 K	89.6	223.7	39.8	355.2	
Cs_2CdI_4	300 - 450 K	46.1	22.0	30.7	74.7	0.977
Cs_2HgI_4	258 - 550 K	41.7	79.5	25.7	146.6	0.983

Next, respective halogen ionicities i estimated from NQR frequencies using eq. (2.20) [7] are listed in Table 4. 4. Here, X1, X2 and X3 correspond to those shown in Fig. 2. 7. X1 is the lowest ionic halogen which directs along a-axis. The ionicity differences between halogens with the highest and the lowest ionicity *i*(X3) - *i*(X1) are also shown in Table 4. 4. The compounds with the IC phase gave the ionicity difference larger than those without the phase. If these differences in ionicity, i.e., those in covalency, of halogens are assumed to be attributable only to the interionic bonding, covalency of Cs-X bonds along *a*-axis in the compounds with the IC phase is considered to be stronger than those without the phase. These facts seem to support the speculation that the one-dimensional interaction along *a*-axis through the covalency of Cs1-X bond affects extremely to the appearance of the IC phase.

Table 4. 4 Halogen Ionicities derived from NQR frequencies for each halogen site in Cs_2MX_4 with the β-K_2SO_4-type structure at room temperature. *i*(X3) - *i*(X1) is equal to the covalency differences between nonequivalent halogen sites, X1 and X3. These differences are attributable to the interionic interaction.

Compound	Halogen Ionicity *i*			Ionicity Difference	Ref.
	i(X1)	*i*(X2)	*i*(X3)	*i*(X3) - *i*(X1)	
Cs_2ZnCl_4	0.796	0.808	0.815	0.019	[8]
Cs_2ZnBr_4	0.770	0.781	0.789	0.019	[8]
Cs_2ZnI_4	0.729	0.741	0.752	0.023	[8]
Cs_2HgCl_4	0.695	0.741	0.748	0.053	[9]
Cs_2CdBr_4	0.759	0.781	0.790	0.031	[10]
Cs_2HgBr_4	0.666	0.704	0.713	0.047	[10]
Cs_2CdI_4	0.716	0.742	0.752	0.036	[11]
Cs_2HgI_4	0.607	0.647	0.679	0.072	[12]

To confirm the validity of this speculation, Cs_2CdBr_4 and Cs_2HgBr_4 are compared because their phase transition temperatures are near to each other. The covalencies of Cs ions showed remarkable temperature dependences in both compounds as shown in Fig. 4. 5. At first, the covalency of Cs2 increases with temperature decrease. Since the interionic interaction in *bc*-plane through Cs2 becomes stronger by the increase of covalency, it can be presumed that the phase of rotational mode of complex anions as the plane wave. With approaching near the N-IC phase transition on cooling, covalency of Cs1 begins to increase steeply as shown in Fig. 4. 5. This result indicates that the interaction along a-axis which is the direction of the IC modulation is getting strong through the Cs1 ions.

Similar temperature dependences of covalency in Cs ions were also observed in Cs_2HgCl_4 as shown in Fig. 4. 6. For Cs_2CdI_4, though it is not clear owing to the measurement in a narrow temperature region studied above the N-IC phase transition, similar temperature behavior in the Cs covalency is considered to be reasonable. On the other hand, in all Cs_2ZnX_4 compounds, the covalencies of Cs2 increased steeply with decreasing temperature, but that of C1 depends on temperature inappreciably.

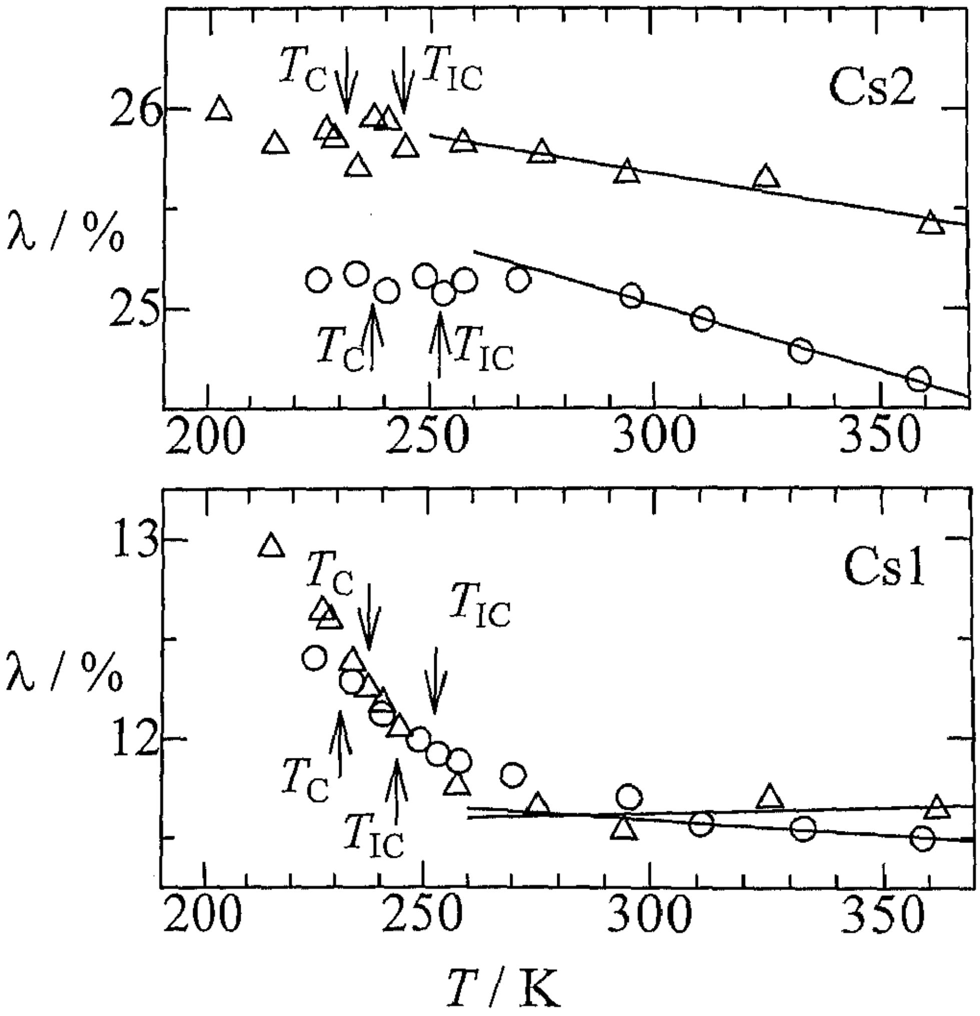

Fig. 4. 5 Temperature dependences of covalencies of Cs1 and Cs2 in both Cs_2CdBr_4 (○) and Cs_2HgBr_4 (△). Solid lines are for guide.

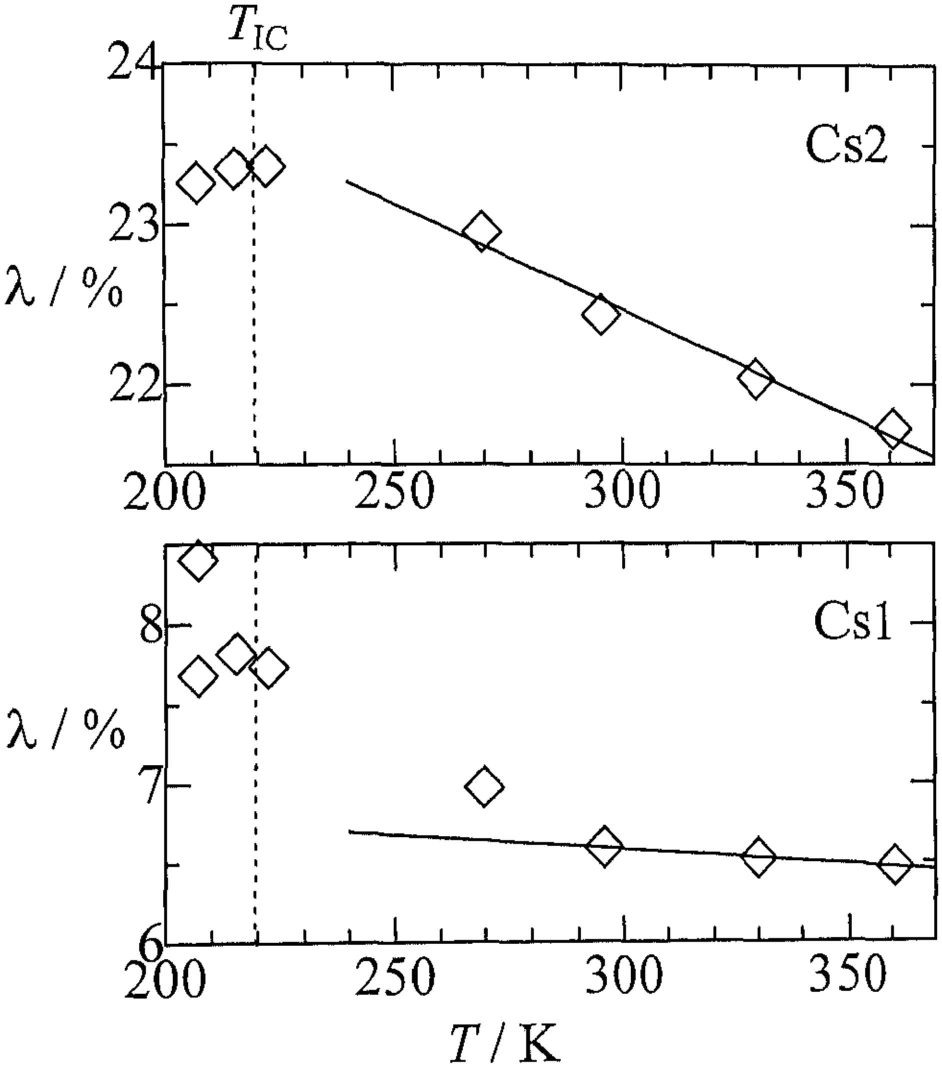

Fig. 4. 6 Temperature dependences of covalencies of Cs1 and Cs2 in Cs_2HgCl_4. Solid lines are for guide.

To trace the temperature change of the local structure around the Cs ions, the temperature dependence of e^2Qq/h for Cs1 was analyzed. The temperature dependences of e^2Qq/h for Cs1 were estimated from ^{133}Cs NMR spectra with the assumption of temperature independent η as shown in Fig. 4. 7. These dependences also showed remarkable differences between Cs_2MX_4 compounds with the IC phase and Cs_2ZnX_4 compounds. For Cs_2MX_4 compounds with the IC phase, the e^2Qq/h values were almost independent of temperature, whereas the e^2Qq/h observed in Cs_2ZnX_4 increased with decreasing temperature. It can be expected that e^2Qq/h increases when the counter ion approaches from the *Z*-direction of the principle axis, while, if counter ions also approach from both directions parallel and perpendicular to Z-direction, e^2Qq/h shows no remarkable increase [13]. On the other hand, the total degree of covalency λ estimated from the NMR chemical shift is the sum of contributions from all direction. Therefore, the temperature change of the local structure around Cs1 can be explained as follow: 1) In Cs_2MX_4 compounds with the IC phase, counter halogen ions approach Cs1 from all direction (Fig. 4. 8 (a)), because λ is getting large with temperature decrease but e^2Qq/h depends on temperature inappreciably. 2) For Cs_2ZnX_4, Cs1 approaches only one complex anion on the single side along the *Z*-direction (Fig. 4. 8 (b)), because e^2Qq/h is getting large with decreasing temperature but λ depends on temperature inappreciably.

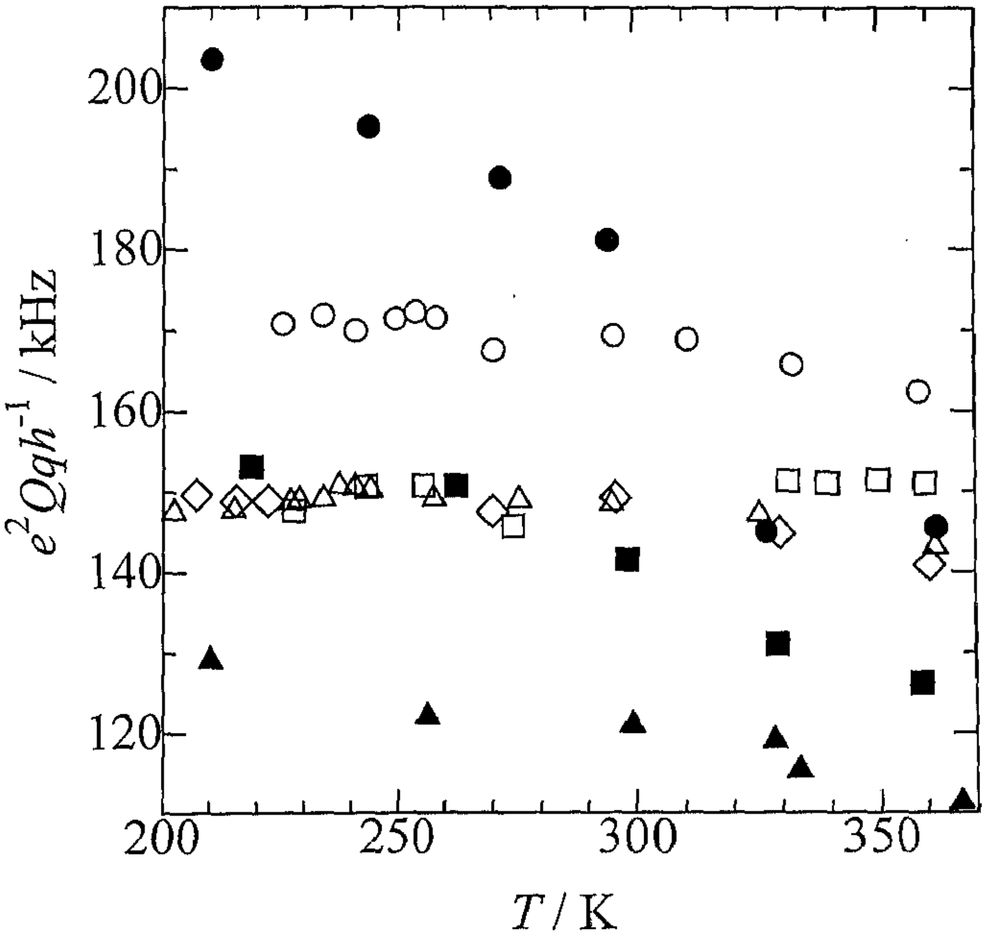

Fig. 4. 7 Temperature dependences of e^2Qq/h of Cs1 in Cs_2MX_4 compounds: Cs_2CdBr_4 (○), Cs_2HgBr_4 (△),and Cs_2CdI_4 (□) and Cs_2HgCl_4 (◇) with IC phases, and Cs_2ZnCl_4 (●), Cs_2ZnBr_4 (▲) and Cs_2ZnI_4 (■) without the phase.

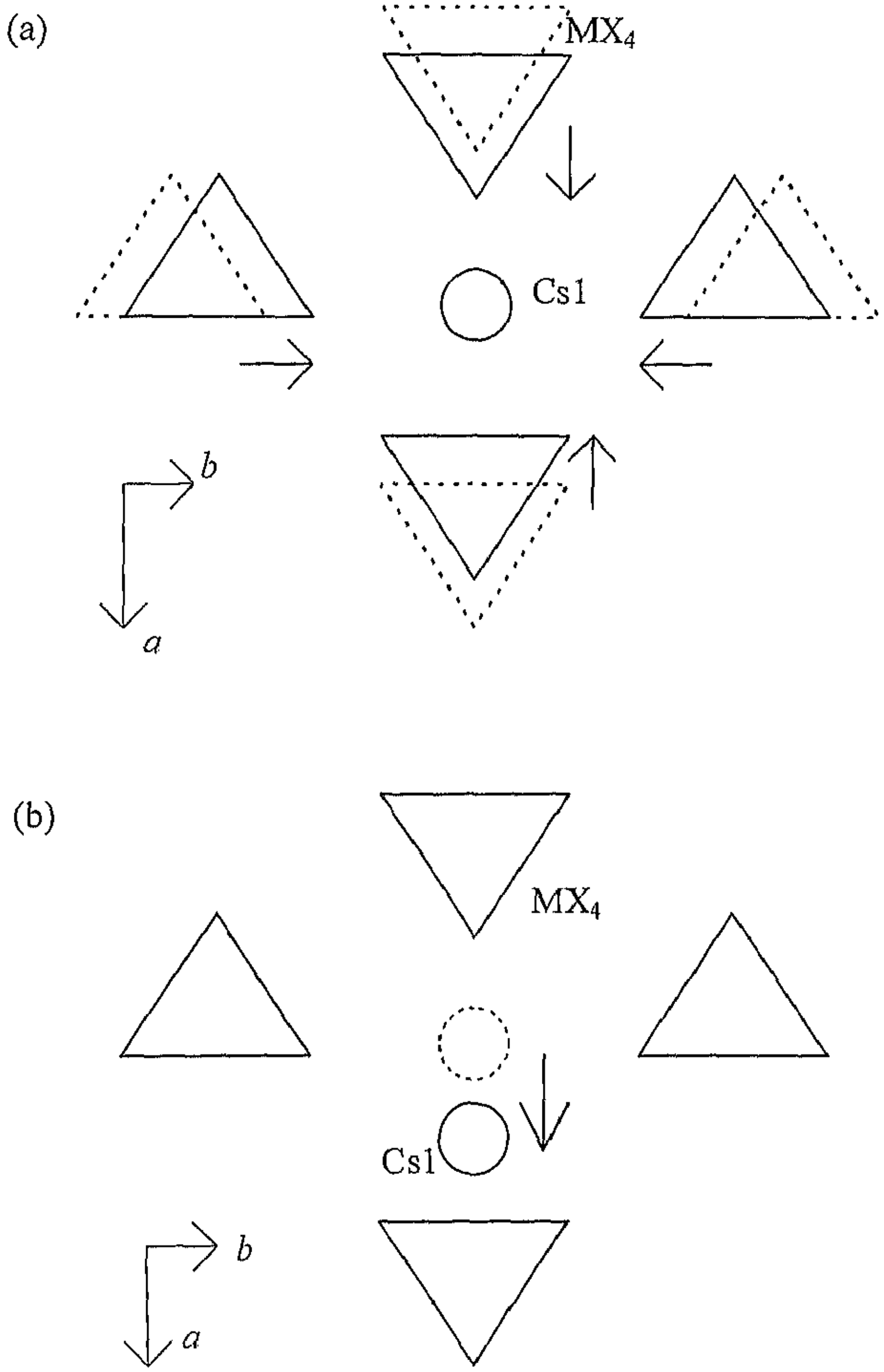

Fig. 4. 8 Changes of the local structure around Cs1 upon cooling as shown by arrows in (a) Cs_2MX_4 compounds with IC phases and (b) Cs_2ZnX_4 without the phase.

Taking into account the above discussion, the microscopic mechanism inducing the IC phase in Cs_2MX_4 compounds with the β-K_2SO_4-type structure can be mentioned as follow: As shown in Fig. 4. 9, tetrahedral complex anions arranging along a-axis tend to take the deviated orientation for the rotational displacement about this axis each other if there is the electrostatic repulsion between halogens at the vertices of anions. On the other hand, it can be expected that these anions tend to take the same orientation each other if partial covalency bonds are formed with Cs1 ions. The competition between the nearest neighbor ferro-type and the 2nd neighbor antiferro-type interactions enables to induce the appearance of the IC modulation upon cooling. In Cs_2MX_4 compounds, it can be expected to be clarified that the nearest neighbor ferro-type interaction is derived from the covalency of Cs1-X bonds, and the 2nd neighbor antiferro-type interaction is from the electrostatic repulsion between halogens at the vertices of complex anions.

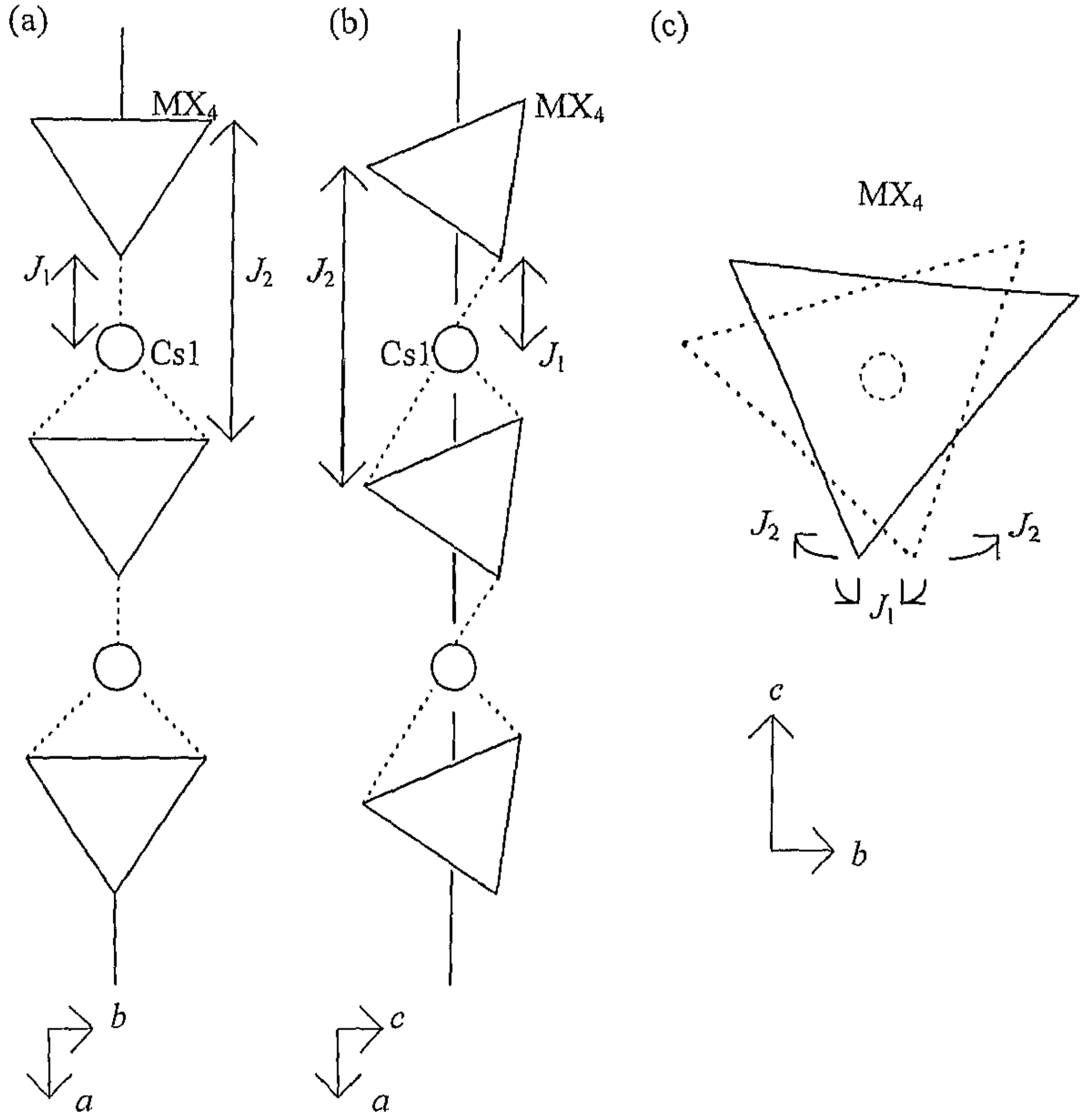

Fig. 4. 9 Illustrations of the IC phase transition mechanisms of Cs_2MX_4 in (a) *ab*-, (b) *ac*-planes and (c) along *a*-axis which is the modulation direction. Circles and triangles are Cs1 and complax anions MX_4, respectively. J_1 is the nearest neighbor ferro-type interaction derived from the covalency of Cs1-X interactions and J_2 is the 2nd neighbor antiferro-type from the electrostatic repulsion between halogens at the vertices of complex anions. The competition between J_1 and J_2 enables to induce the appearance of the IC modulation upon cooling.

4.4 Conclusion

From the present study, it can be concluded that the one-dimensional interaction along *a*-axis due to the covalency of Cs1-X bond affects markedly to the appearance of the IC phase in Cs_2MX_4 compounds with the β-K_2SO_4-type structure. In Cs_2ZnX_4, since Cs1 approaches only one complex anion on the single side along the *Z*-direction, no one-dimensional network of the interaction is expected to be formed. But in Cs_2MX_4 compounds with the analogous IC phase, the one-dimensional network can be formed because counter halogen ions approach Cs1 from the both sides along *a*-axis,.

From the analysis of the experimental results, it can be anticipated that interactions in Cs_2MX_4 compounds with the analogous IC phases showed the temperature dependences as follows: The covalency of Cs2 increases with temperature decrease. The interaction, which determines phases of rotational mode of complex anions in *bc*-plane, is formed through the Cs2 ions. With approaching near the N-IC phase transition on cooling, the covalency of Cs1 begins to increase steeply. The interaction along a-axis which is the direction of the IC modulation is getting strong through the Cs1 ions.

Considering the only one-dimensional interaction along a-axis, tetrahedral complex anions arranging along *a*-axis tend to take the deviated orientation for the rotational displacement about this axis each other, if the antiferro-type electrostatic repulsion is present between halogens at the vertices of anions. On the other hand, these anions tend to take the same orientation each other, which is the ferro-type interaction, in case partial covalency bonds are formed with Cs1 ions. The competition between the nearest neighbor ferro-type and the 2nd neighbor antiferro-type interactions enables to induce the appearance of the IC modulation upon cooling. In Cs_2MX_4 compounds, it can be expected that the nearest neighbor ferro-type interaction is derived from the covalency of Cs1-X bonds, and the 2nd neighbor antiferro-type is from the electrostatic repulsion between halogens at the vertices of complex anions.

References in Chapter 4

[1] P. Bak, *Rep. Prog. Phys.*, **45** (1982) 587.

[2] T. Janssen, *Incommensurate Phases in Dielectrics 1. Fundamentals*, ed. R. Blinc and A. P. Levanyuk, North Holland, Amsterdam, 1986, Chap. 3.

[3] H. Z. Cummins, *Phys. Rep.*, **185** (1990) 211 and references therein.

[4] W. Selke, *Phase Transition and Critical Phenomena*, Vol. 15, ed. C. Domb and J. L. Lebowitz, Academic Press, London, 1992, Chap. 1.

[5] R. G. Barnes and W. V. Smith, *Phys. Rev.*, **93** (1954) 95.

[6] H. Nakayama, N. Nakamura and H. Chihara, *Bull. Chem. Soc. Jpn.*, **60** (1987) 99.

[7] C. H. Townes and B. P. Dailey, *J. Chem. Phys.*, **23** (1955) 118.

[8] D. E. Scaife, *Aust. J. Chem.*, **24** (1971) 1315.

[9] A. A. Boguslavskii, R. Sh. Lotfullin, M. V. Simonov, V. V. Kirilenko, V. I. Pakhomov and A. Ya. Mikhailova, *Sov. Phys. Solid State*, **27** (1985) 321.

[10] S. Plesko, P. Kind and H. Arend, *Phys. Stat. Sol. A*, **61** (1980) 87.

[11] E. V. Shemetov, K. S. Aleksandrov, I. P. Aleksandrova and S. V. Primak, *Phys. Stat. Sol. A*, **104** (1987) K89.

[12] A. A. Boguslavskii, D. L. Zagorskii, R. Sh. Lotfulin, V. I. Pakhomov, V. V. Kirilenko and G. K. Semin, *Russ. J. Inorg. Chem.*, **34** (1989) 1023.

[13] F. Seitz and D. Turnbull eds., *Solid State Physics*, Suppl. 1, T. P. Das and E. L. Hahn, "*Nuclear Quadrupole Resonance Spectroscopy*", Academic Press, New York, 1958.